ORIGINAL PAPER

Cytotoxic Activity and DNA-binding Properties of Xanthone Derivatives

Rui Shen · Peng Wang · Ning Tang

Abstract In this study, the interactions of different groups substituted xanthone derivatives with calf thymus DNA (ct DNA) have been investigated by spectrophotometric methods and viscosity measurements. Results indicate that xanthone derivatives can intercalate into the DNA base pairs by the plane of xanthone ring and the various substituents may influence the binding affinity with DNA according to the calculated quenching constant values and the melting temperature of DNA. Furthermore, three tumor cell lines including esophagus squamous cancer cell line (ECA109), stomach cancer cell line (SGC7901) and lung cancer cell line (GLC-82) have been used to evaluate the cytotoxic activities of xanthone derivatives by MTT (microculture tetrazolium) method. Analysis show that the oxiranylmethoxy or piperidinylethoxy substituted xanthones exhibit more effective cytotoxic activity against three cancer cells than the other substituted xanthones. The effects on the inhibition of tumor cells in vitro agree with the studies of DNA-binding.

Keywords Xanthone derivatives · DNA-binding · Cytotoxic activity

R. Shen (✉) · P. Wang
College of Pharmacy, Nankai University,
Tianjin 300071, People's Republic of China
e-mail: shenr05@lzu.cn

N. Tang
College of Chemistry and Chemical Engineering,
Lanzhou University,
Lanzhou 730000, People's Republic of China

Introduction

Xanthones are secondary metabolites commonly occurring in a few higher plant families and microorganisms. They have a large variety of biological and pharmacological activities including antihypertensive, antioxidative, antithrombotic, and anticancer activity, etc. [1–5], based on their diverse structures (Fig. 1). Accordingly, many scientists apply themselves to isolate or synthesize these compounds for the development of prospective new drug candidates. Especially, the effective inhibitory activity against human cancer cell lines has attracted considerable attention [6–10]. The preliminary work has highlighted the high potentials of xanthones as a promising building motif for the development of a new class of potent anticancer drugs.

Numerous biological experiments have demonstrated that deoxyribonucleic acid (DNA) is the primary intracellular target of anticancer drugs due to the interaction between small molecules and DNA, which cause DNA damage in cancer cells, inhibiting the division of cancer cells and resulting in cell death [11, 12]. Up to present, the systematic studies of the interaction of the xanthone compounds with DNA have been reported rarely [6, 7, 9], and their structure-activity relationships remain unestablished in the xanthones system. Lin and coworkers report that 2,3-epoxypropoxy substituted xanthones have efficiently prohibited growth of cancer cells and xanthone possessing two 2,3-epoxypropoxy groups at 3 and 5 position showed most active anticancer activity in the series prepared [13, 14]. The structural features inherent in xanthone derivatives make us aware that the different substitute groups in xanthones may influence significantly to the biological activity.

With this rational in mind, we have investigated the binding mode and affinity of xanthone derivatives **1**–**6**
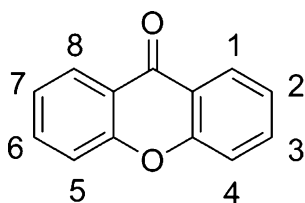
Fig. 1 Nucleus of xanthone

(Fig. 2) to DNA and their effect on the growth of three human cancer cell lines, ECA109 (esophagus squamous cancer), SGC7901 (stomach cancer) and GLC-82 (lung cancer) in vitro. The primary aim of these experiments are expected to gain some insight into the effect of structure factor on the binding of various substituted xanthones to DNA and offer an impetus for designing newer DNA directed therapeutic agents.

Experimental

Materials

Xanthone derivatives **1–6** were prepared according to the literatures with some improvement [15, 16]. Other chemicals were reagent grade and were used without further purification. Calf thymus DNA (ct DNA) and ethidium bromide (EB) were obtained from Sigma Chemical Co.

Measurements

Mass spectra (MS) were performed on a VG ZAB-HS instrument and ^{1}H NMR spectra were recorded using a Varian Mercury Plus 400 spectrometer. The UV-Vis absorption spectra were recorded using a Varian Cary 100 spectrophotometer and the fluorescence emission spectra were recorded using a Hitachi F-4500 spectrofluorophotometer, respectively.

The thermal denaturization of ct DNA was carried out in doubly distilled water buffer containing 1 mM Tris (Tris = trihydroxymethyl aminomethane), 0.1 mM Na_2EDTA (EDTA = ethylenediamine tetraacetic acid) and

adjusted to pH 7.4 with HCl; the other measurements involving the interaction of xanthone derivatives with ct DNA were carried out in doubly distilled water buffer containing 5 mM Tris, 50 mM NaCl and adjusted to pH 7.4 with HCl.

UV-Vis spectrometer was employed to check a solution of ct DNA purity (A_{260}: A_{280} > 1.80) and concentration (ε = 6,600 $M^{-1}cm^{-1}$ at 260 nm) in the buffer [17, 18]. The xanthone compounds were first dissolved in a minimum amount of ethanol (0.05% of the final volume), and then diluted with Tris-HCl buffer at concentration 5 μM.

Preparation of xanthone derivatives **1–6** [15, 16]

The synthetic route of dihydroxylxanthone **1** and their alkoxy derivatives **2–6** is shown in Fig. 2. Compound **1** was synthesized in 38% yield from the condensation of salicylic acid with phloroglucinol in the presence of anhydrous zinc chloride and phosphorus oxychloride as a condensing agent. Alkylation of **1** with alkyl halides in acetone or DMF afforded **2–6** in moderate to good yields (50–85%). All the crude products were purified by chromatography on a silicagel column and recrystallized to afford **1–6** as yellow solids.

1, 3-Dihydroxyxanthone (1). Yield 38.25%, MS: 228.1[M], ^{1}H NMR (400 MHz, Acetone-d6): δ 8.23–8.20 (dd, 1 H), 7.89–7.84 (dt, 1 H), 7.57–7.55 (d, 1 H), 7.51–7.46 (t, 1 H), 6.47–6.46 (d, 1 H), 6.30–6.29 (d, 1 H) ppm.

1-Hydroxy-3-ethoxyxanthone (2). Yield 85.16%, MS: 256.0 [M], ^{1}H NMR (400 MHz, $CDCl_3$): δ 12.87 (s, 1 H), 8.28–8.23 (dd, 1 H), 7.77–7.68 (m, 1 H), 7.46–7.38 (m, 2 H), 6.44–6.35 (dd, 2 H), 4.16–4.12 (dd, 2 H), 1.51–1.44 (t, 3 H) ppm.

1-Hydroxy-3-butoxyxanthone (3). Yield 80.28%, MS: 284.0 [M], ^{1}H NMR (400 MHz, $CDCl_3$): δ 12.86 (s, 1 H), 8.29–8.24 (dd, 1 H), 7.77–7.69 (m, 1 H), 7.46–7.38 (m, 2 H), 6.44–6.35 (dd, 2 H), 4.10–4.04 (t, 2 H), 1.83–1.79 (m, 2 H), 1.55–1.50 (m, 2 H), 1.04–0.97 (t, 3 H) ppm.
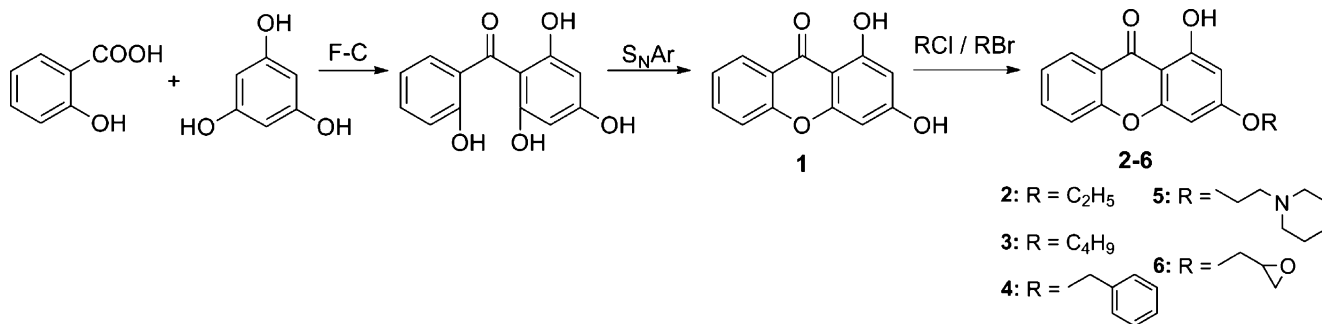

Fig. 2 Synthetic route for xanthone derivatives **1–6**

1-Hydroxy-3-benzyloxyxanthone (4). Yield 74.21%, MS: 318.0 [M], ^{1}H NMR (400 MHz, CDCl$_3$): δ 12.89 (s, 1 H), 8.29–8.25 (dd, 1 H), 7.77–7.69 (m, 1 H), 7.46–7.36 (m, 7 H), 6.54–6.44 (dd, 2 H), 5.18 (s, 2 H) ppm.

1-Hydroxy-3-(2-(1-piperidinyl)ethoxy)xanthone (5). Yield 69.61%, MS: 339.1 [M], ^{1}H NMR (400 MHz, CDCl$_3$): δ 12.86 (s, 1 H), 8.28–8.24 (dd, 1 H), 7.77–7.68 (m, 1 H), 7.46–7.34 (m, 2 H), 6.46–6.36 (dd, 2 H), 4.26–4.20 (t, 2 H), 2.88–2.82 (t, 2 H), 2.56 (br, 4 H), 1.65–1.63 (br, 4 H), 1.49–1.47 (br, 2 H) ppm.

1-Hydroxy-3-(2-oxiranylmethoxy)xanthone (6). Yield 51.41%, MS: 283.9 [M], ^{1}H NMR (400 MHz, CDCl$_3$): δ 12.89 (s, 1 H), 8.27–8.25 (dd, 1 H), 7.75–7.71 (m, 1 H), 7.46–7.26 (m, 2 H), 6.48–6.37 (dd, 2 H), 4.37–4.34 (m, 1 H), 4.04–3.99 (m, 1 H), 3.42–3.39 (m, 1 H), 2.97–2.95 (m, 1 H), 2.81–2.79 (m, 1 H) ppm.

DNA interactions

The competitive binding experiment was carried out by maintaining the EB and ct DNA concentration at 2 μM and 30 μM, respectively, while increasing the concentration of xanthone derivatives. Fitting was completed using an Origin 6.0 spreadsheet, where values of the quenching constant K_q were calculated. Fluorescence spectra experiment was performed by fixing the xanthones concentration as constant at 5 μM while varying the concentration of ct DNA.

Viscosity experiments were carried on an Ubbelodhe viscometer, immersed in a thermostated water-bath maintained to 35.0±0.5 °C. Titrations were performed for EB or xanthone derivatives (1–6 μM), and the compounds were introduced into DNA solution (50 μM) present in the viscometer. Flow time was measured with a digital stopwatch. The average time was calculated from the triplicate measurement results.

Thermal denaturization experiments were performed on a UV-Vis spectrophotometer equipped with a Peltier temperature controller in 1 mM Tris-HCl buffer. The temperature of the cell containing the cuvette was ramped from 50 °C to 100 °C at 1 °C /min rate, and the absorbance at 260 nm was measured every 2 °C. The T_m values were determined from the maximum of the first derivative or tangentially from the graphs at midpoint of the transition curves. ΔT_m values were calculated by subtracting T_m of the compound with ct DNA from T_m of the free ct DNA.

Cell culture and cytotoxicity assay

Cells were supplied by the School of Pharmacy, Lanzhou University (Lanzhou, China). Cells were routinely kept in RPMI-1640 medium supplemented with 10% fetal bovine serum, penicillin G (100 U/mL) and streptomycin (100 μg/mL) at 37 °C in a humidified atmosphere containing 5% CO$_2$. After a confluent cell layer was formed, the cells were harvested from the adherent cultures using 0.25% trypsin + 0.02% EDTA in phosphate buffered saline or D-Hank's buffer for 5 min. Suspensions were adjusted to cell densities of 5×10^4 cells/mL in order to ensure exponential growth throughout drug exposure. Aliquots of these suspensions were seeded into 96-well microcultures (90 μL/well). After incubation for 24 h, cells were exposed to the tested compounds of serial concentrations. Xanthone derivatives were dissolved in ethanol and diluted with RPMI-1640 to the required concentrations prior to use. After addition, the different concentration of xanthones (10 μL/well) and incubation for 68 h, 10 μL of aqueous MTT solution (5 mg/mL) was added to each well, and the cells were incubated continually for another 4 h. The medium and MTT mixtures were removed and the formazan crystals were dissolved in 100 μL DMSO/cell. The absorbance of each cell at 570 nm was determined by analysis with a microplate spectrophotometer (EL$_X$800, U.S.A.), and the percentage cell viability was determined by dividing the average absorbance of each column of xanthones-treated wells by the average absorbance of the control wells. The growth inhibitory rate of treated cells was calculated by $(OD_{control} - OD_{test})/OD_{control} \times 100\%$. The IC$_{50}$ values were determined by plotting the percentage viability versus concentration on a logarithmic graph and reading off the concentration at which 50% of cells remain viable relative to the control. Each experiment was repeated at least three times to get the mean values.

Results and discussion

Competitive binding experiment

By measuring the ability of a compound to affect the ethidium bromide (EB) fluorescence intensity in the DNA-EB adduct, the binding mode and affinity of the compound for DNA can be determined. If a compound can replace EB from DNA-EB, the fluorescence of the solution will decrease due to the fact that free EB molecules are readily to be quenched by the surrounding water molecules [19]. Figure 3 shows the emission spectra of DNA-EB system upon the increasing amount of xanthone derivatives. The emission intensity of DNA-EB system at 587 nm decreases as the concentration of xanthones increased and an isobathic point appears around 550–560 nm for the alkoxy substituted xanthones. This indicates that xanthone derivatives could displace EB from the DNA-EB system and induce the translocation of EB from a hydrophobic environment to an aqueous environment [20]. Such a
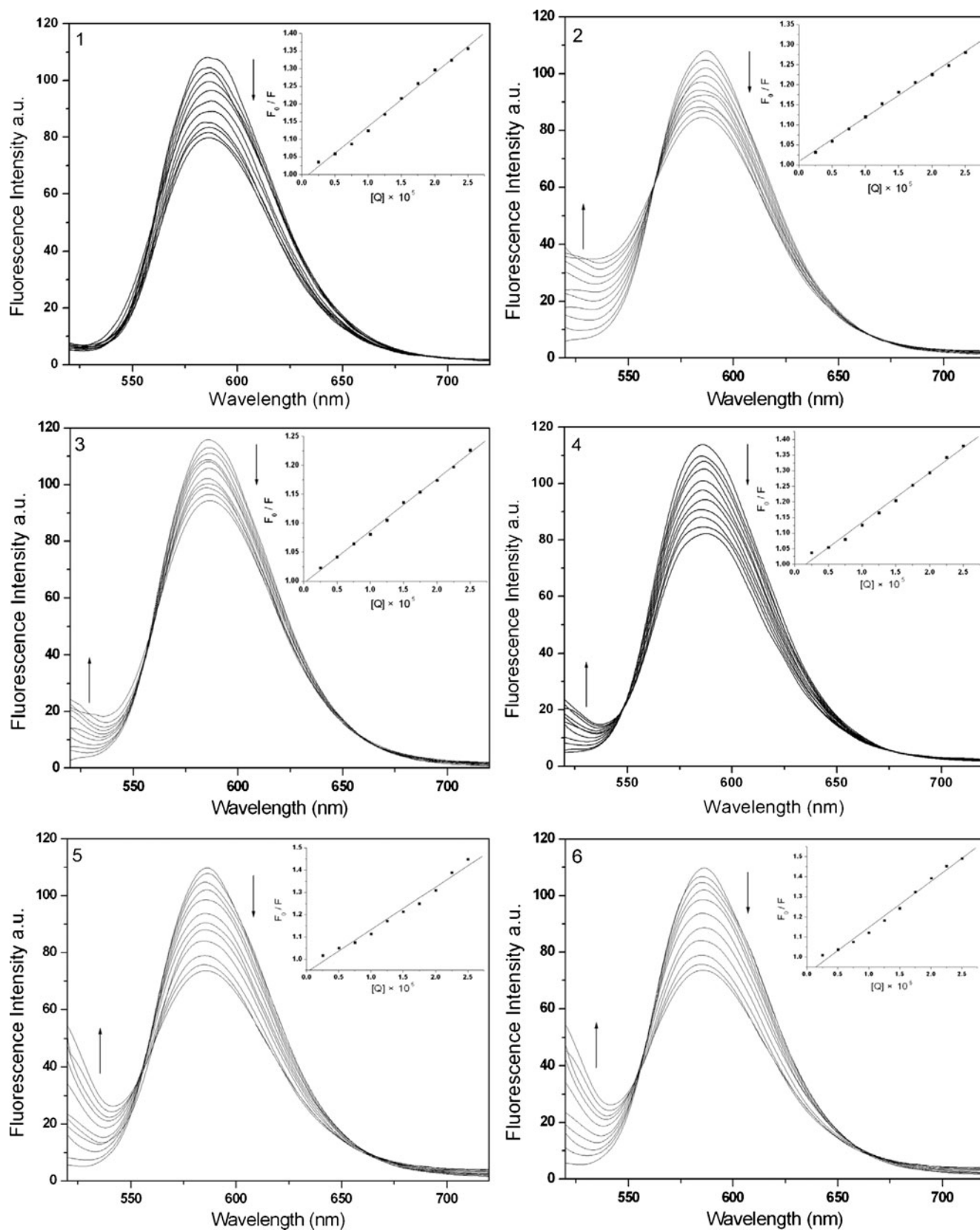
Fig. 3 Fluorescence emission spectra of DNA-EB in the absence and presence of increasing amounts of xanthone derivatives **1**–**6** (λ_{ex}= 500 nm, λ_{em}=520–720 nm) C_{EB}=2 μM, C_{DNA}=20 μM, $C_{compound}$=0, 2.5, 5, 7.5, 10, 12.5, 15, 17.5, 20, 22.5, 25 μM. The inset is Stern-Volmer quenching plots

Table 1 The K_q and IC_{50} values of xanthone derivatives **1**–**6** in EB displacement experiments[a]

	1	2	3	4	5	6
$K_q \times 10^4$	1.51	1.09	0.89	1.59	1.91	2.29
$IC_{50} \times 10^{-4}$ (M)	0.66	0.92	1.12	0.63	0.52	0.43

[a] IC_{50} represents the concentration of quencher that is required for 50% quenching

characteristic change is often observed in intercalative DNA interactions [21].

According to the classical Stern-Volmer Eq. (1) [22]:

$$F_0/F = 1 + K_q[Q] \tag{1}$$

where F_0 and F represent the emission intensity in the absence and presence of quencher, respectively, K_q is a linear Stem-Volmer quenching constant and [Q] is the quencher concentration. The quenching plots illustrate that the quenching of EB bound to DNA by xanthone derivatives are in good agreement with the linear Stern-Volmer equation (Fig. 3, inset). In the plots of F_0/F versus [Q], K_q is given by the ratio of the slope to the intercept. The K_q and IC_{50} values for the xanthones are summarized in Table 1, so the order of the binding affinity is **3** < **2** < **1** < **4** < **5** < **6** by comparing quenching constant values. Moreover, as these changes indicate only one quenching process, it may be concluded that the compounds bind to DNA solely by intercalation mode.

Because EB is useful as a DNA structure probe, further support for xanthone derivatives binding to DNA by intercalation mode is shown in Fig. 4. The maximal absorption of EB at 480 nm decreased and shifted to 525 nm in the presence of DNA, which is characteristic of intercalation. The dotted curve in Fig. 4 shows the absorption spectrum of a solution containing EB, xanthones and DNA. It is found that the absorption at about 525 nm increased in comparison with that shown in dashed curve of Fig. 4. It could result from two reasons: (1) EB bound to the compounds strongly, resulting in the decrease of the amount of EB intercalated into DNA; (2) there exist competitive intercalation between the compounds and EB with DNA, so releasing some free EB from DNA-EB complex [23]. However, the former reason could be precluded because no new absorption peak was seen.

Fluorescence spectra experiment

In Tris-HCl buffer, xanthone derivatives have fluorescence around 410 nm when excited at 305 nm. If DNA solution is added to the xanthones solution, enhanced fluorescence is observed when excited under the given conditions. Figure 5

shows the fluorescent emission spectra of xanthone derivatives in the presence and absence of DNA. The results suggest that the xanthones can be protected efficiently from solvent water molecules by the hydrophobic environment inside the DNA helix. This indicates that the xanthones can insert between DNA base pairs deeply, which is consistent with the above competitive binding experiment results. Since the hydrophobic environment inside the DNA helix reduces the accessibility of solvent water molecules to the compound and the compound mobility is restricted at the binding site, a decrease of the vibrational modes of relaxation results. The binding of the xanthones to DNA leads to a marked increase in emission intensity, which also agrees with those observed for other intercalators [24].

Viscosity measurements

Optical photophysical probes generally provide necessary, but not sufficient, clues to support a binding model. Hydrodynamic measurements that are sensitive to length change (i.e. viscosity and sedimentation) are regarded as the least ambiguous and the most critical tests of binding model of small molecule to DNA in solution in the absence of crystallographic structural data. A classical intercalation model results in lengthening the DNA helix as base pairs are separated to accommodate the binding small molecules, leading to the increase of DNA viscosity. In contrast, a partial and non-classical intercalation of small molecules could bend or kink the DNA helix, reduce its effective length and, concomitantly, its viscosity [25, 26].

To confirm the above inferences, viscosity measurements are carried out and the results are presented as $(\eta/\eta_0)^{1/3}$ versus binding ratio, where η is the viscosity of DNA in the presence of xanthone derivatives, and η_0 is the viscosity of DNA alone. Viscosity values are calculated from the observed flow time of DNA-containing solution corrected from the flow time of butter alone (t_0), $\eta = t - t_0$ [27, 28]. As can be seen from Fig. 6, EB, compound **5** and **6** can increase the relative viscosity of DNA greatly, and the extent of the viscosity increase caused by EB is more obvious, which is consistent with the literature reports [29, 30]. Upon increasing the amounts of compound **1**, **2**, **3** and **4**, the relative viscosity of DNA increases steadily similarly to the behavior of EB, compound **5** and **6**. The increased degree of viscosity, which may depend on the binding affinity to DNA, follows the order of **3** < **2** < **1** < **4** < **5** < **6** < EB. These agree with the results of the competitive binding experiment. The results demonstrate that the xanthones can intercalate between adjacent DNA base pairs, causing an extension in the helix, and the binding affinity of compound **5** and **6** is higher than that of the other compounds.
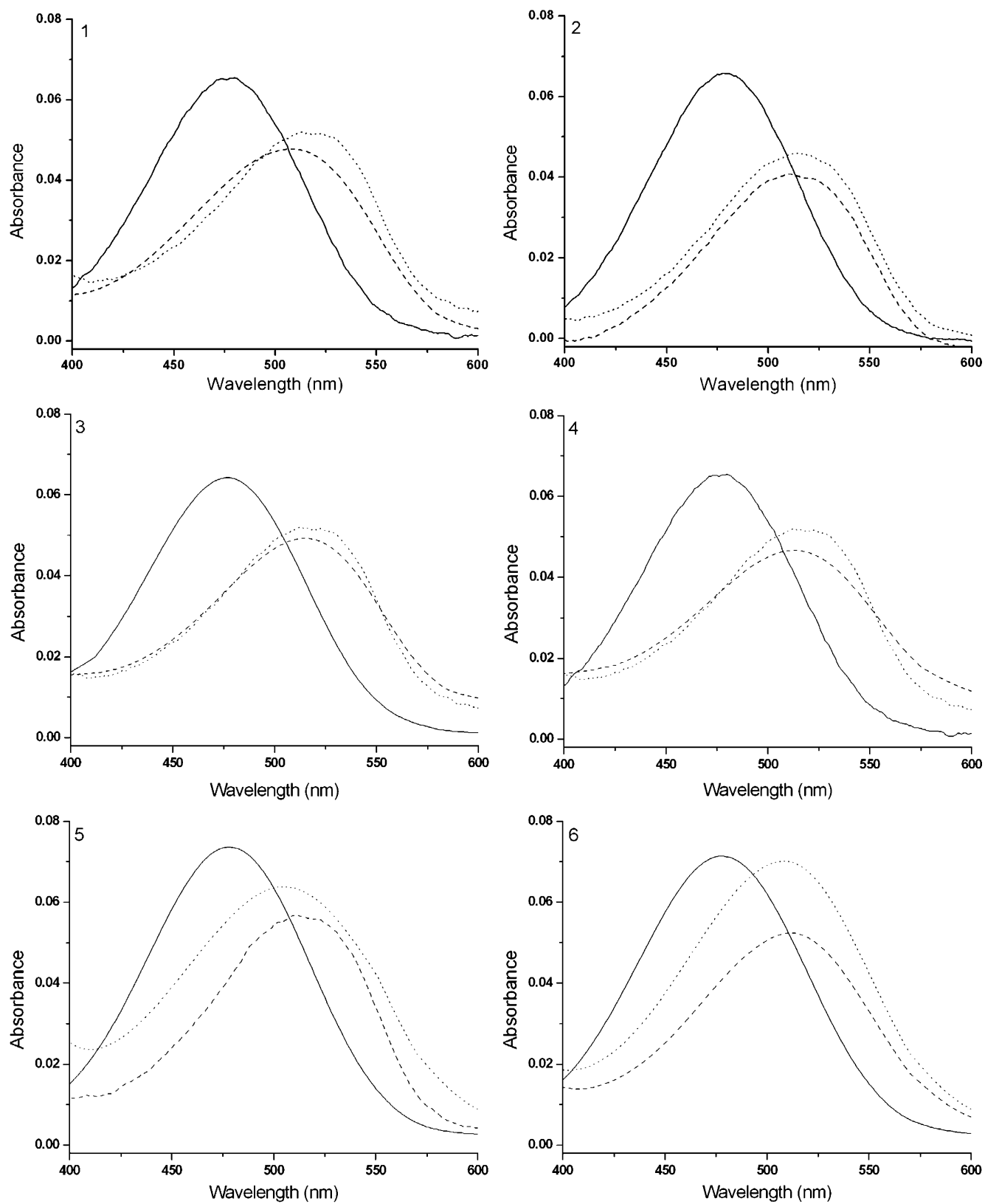
Fig. 4 The visible absorption spectra of 10 μM EB (solid curve); 10 μM EB + 10 μM DNA (dashed curve); 10 μM EB +10 μM DNA + 5 μM xanthone derivatives **1–6** (dotted curve)
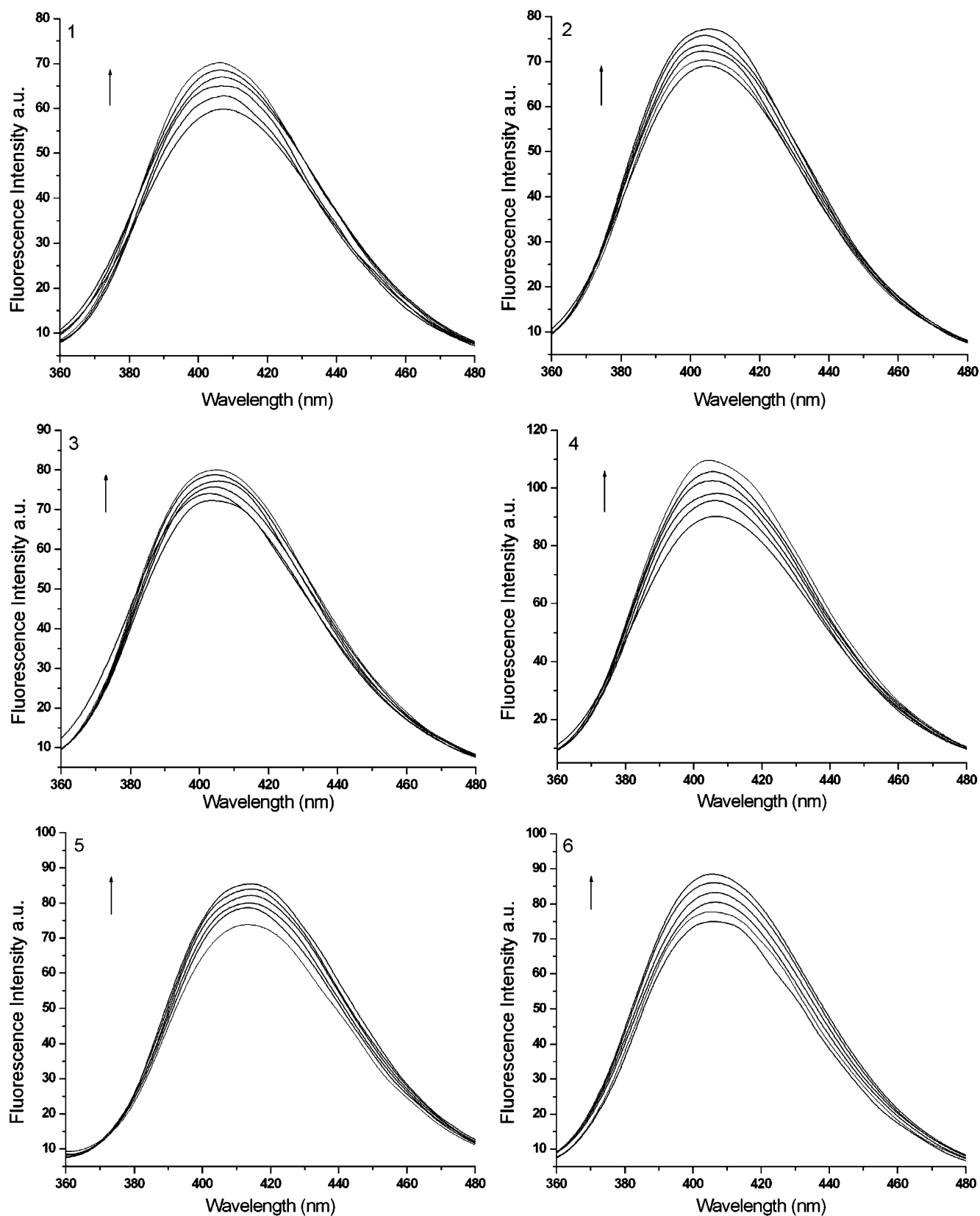
Fig. 5 Fluorescence emission spectra of xanthones in the presence of increasing amounts of ct DNA. (λ_{ex}=305 nm, λ_{em}=360–480 nm) C_{Cu}= 5 μM, C_{DNA}=0, 5, 10, 15, 20, 25 μM
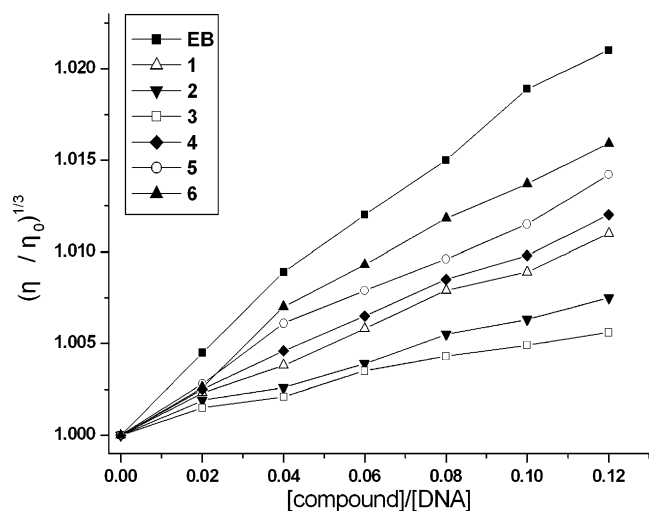
Fig. 6 Effects of increasing amounts of EB (■), **1** (△), **2** (▼), **3** (□), **4** (♦) **5** (○) and **6** (▲) on the relative viscosities of ct DNA ([DNA] = 50 μM), shown as a function of the concentration ratios of [Compound]/[DNA]. η is the viscosity of DNA in the presence of compounds and η_0 is the viscosity of DNA alone

Fig. 7 Thermal denaturization curves of ct DNA ([DNA] = 50 μM) at the concentration ratios of [Compound]/[DNA] = 1/10. (DNA (▽), DNA+**1** (△), DNA+**2** (□), DNA+**3** (▲), DNA+**4** (▼), DNA+**5** (○) and DNA+**6** (■))

Thermal denaturization of DNA

Intercalation of small molecules into the double helix is known to increase the helix melting temperature, the temperature at which the double helix denatures into single-strand DNA. The extinction coefficient of DNA bases at 260 nm in the double-helical form is much less than that in the single strand form, hence, melting of the helix leads to an increase in the absorption at this wavelength. Thus, the helix to coil transition temperature can be determined by monitoring the absorbance of the DNA bases at 260 nm as function of temperature [18, 31–33]. The thermal denaturation profiles of ct DNA in the absence and presence of xanthone derivatives **1–6** are shown in Fig. 7. A_0, A_f and A are the initial absorbance, the final absorbance and the apparent absorbance, respectively. The A_f maxima is about 0.51. In the absence of the xanthones, ct DNA shows a main transition at T_m=69.3 °C. A slight increase in the melting temperature is observed in the presence of **1**, **2** and **3**, while the T_m of ct DNA is distinctly increased upon addition of **4**, **5** and **6** (Table 2). Compared with some DNA intercalators [34], the large increased ΔT_m suggest an intercalative binding of xanthones to DNA. This result is also consistent with the notion that the compounds binds to DNA by intercalation mode and the intercalative binding of the compound **5** and **6** is stronger than that of the others.

Cell culture and cytotoxicity assay

To evaluate the potential cytotoxic activity of xanthone derivatives **1–6**, three human cancer cell lines including
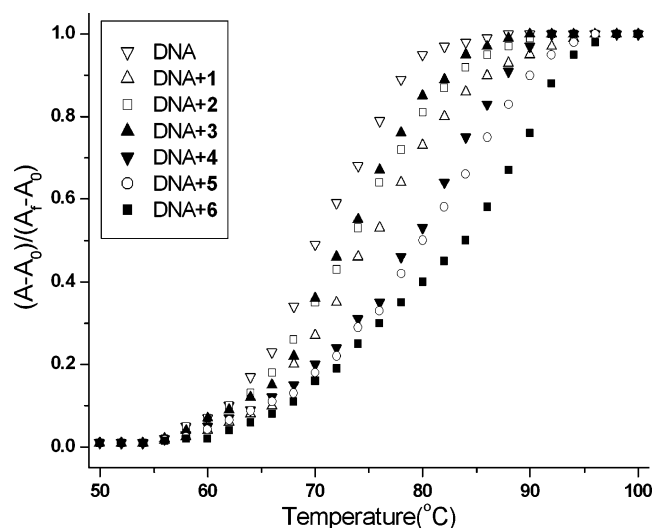
ECA109 (esophagus squamous cancer), SGC7901 (stomach cancer) and GLC-82 (lung cancer) are incubated for 72 h with varying concentrations of them and the cell viability is determined by the MTT assay in vitro.

The cell viability is decreased in response to xanthone derivatives **1–6** in a dose-dependent manner as illustrated in Fig. 8. These compounds exhibit certain cytotoxic activity against three human tumor cell lines. The results demonstrate that the tree tumor cell lines are susceptible to the xanthones. It may because the compounds intercalate into the base group pairs of DNA, which induce damage to DNA in the cancer cells, inhibiting the division of cancer cells and resulting in cell death [11]. Combining with the DNA-binding experiment, it's possible that the different substitute groups could influence the electron cloud density change of xanthone ring by different level. And the increased aromaticity and the concentrated negative charge centers would cause the molecular shows a stronger polarity. The molecular polarity changes relate to DNA binding affinity. The flexible chain with active group linked at rigid xanthone plane may enhance the DNA binding affinity and facilitate the DNA selective binding, which imply that the various substituent flexible side chains in xanthone derivatives might contribute to the

Table 2 The ΔT_m values of ct-DNA in the presence of xanthone derivatives **1–6**

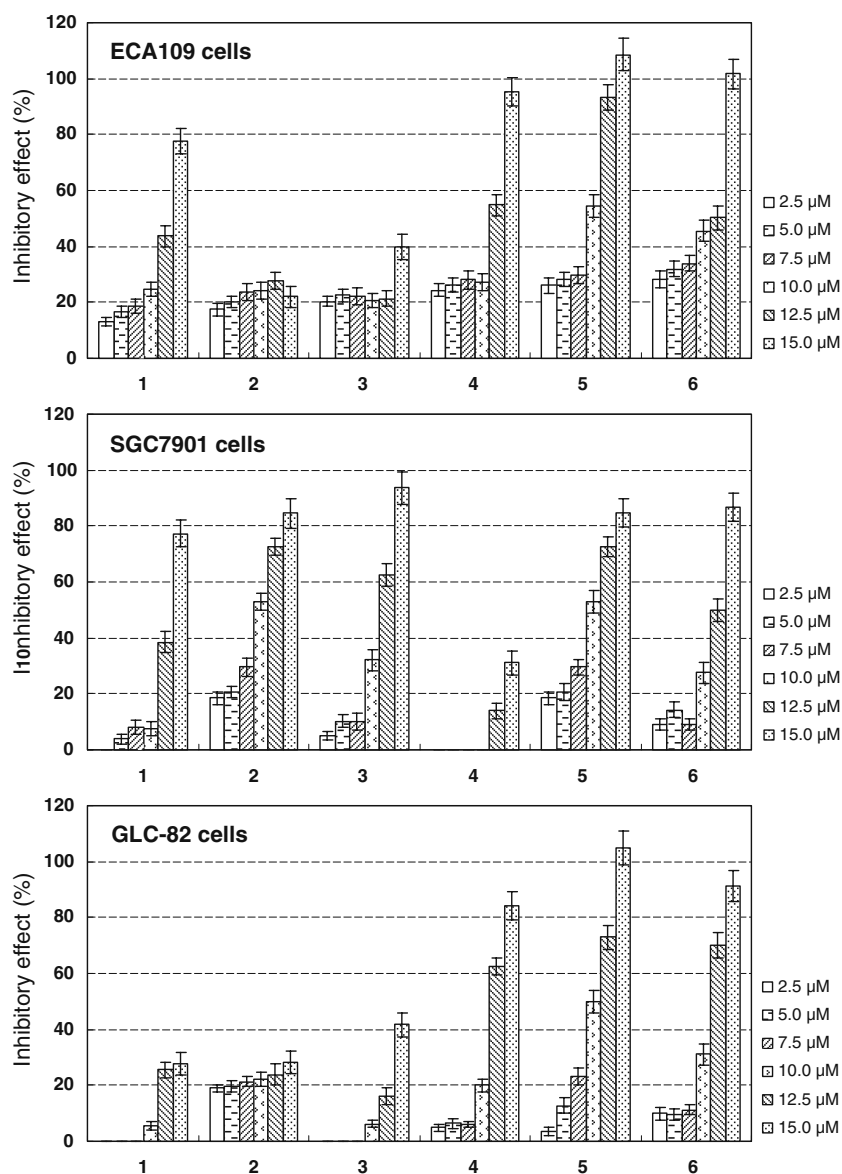| Xanthones derivatives	1	2	3	4	5	6
ΔT_m (°C)	5.8	3.8	3.5	9.8	10.9	14.6

Fig. 8 Cytotoxicities of xanthone derivatives **1–6** against various human cancer cells

increase of their anticancer activity or to the decrease of their toxicity.

Comparing to the IC_{50} values of xanthone derivatives **1–6** against various human cancer cells, the oxiranylmethoxy or piperidinylethoxy substituted xanthones have efficiently prohibited growth of three cancer cells; the other group substituted xanthones have inhibited growth of different cancer cells (Table 3). This suggests that the cytotoxic activity of the same compound against one tumor cell line differ from another. It is likely that the exact action mechanisms of xanthones against tumor cell lines are different from each other because of the multiple

Table 3 The IC_{50} values of xanthone derivatives **1–6** against various human cancer cells

IC_{50} (μ M) Cell	1	2	3	4	5	6
ECA109 (esophagus)	13.87	>100	>100	9.58	6.42	7.84
SGC7901 (stomach)	16.78	8.25	10.38	>100	8.17	12.06
GLC-82 (lung)	98.49	>100	67.35	12.06	8.25	10.07

structures and compositions in various tumor cell lines. The complicated mechanisms about the effect of the compounds on the tumor cells are currently under the way.

Conclusion

The interaction mode between DNA and a series different substituted xanthones have been investigated by spectrophotometric methods and viscosity measurements. The results suggest that xanthones can intercalate into the base group pairs of DNA because of the good planarity of their ring. They all have strong binding affinity with DNA. Comparing the binding extents of them, it is concluded that binding affinity of oxiranylmethoxy or piperidinylethoxy substituted xanthones is stronger than the other group substituted xanthones. The result of inhibitory effect in vitro is consistent with the result of DNA binding study. And each compound would show the cytotoxic activity varying according to the various tumor cells. We conclude that the xanthones intercalate between DNA base pairs and cause DNA damage in cancer cells, thus inhibiting the division of cancer cells. Information obtained from the present work provides evidence for the nature of the binding of the xanthones to DNA and is expected to offer further impetus for designing newer probes for DNA structure and novel therapeutic agents that are directed at DNA.

References

1. Recanatini M, Bisi A, Cavalli A, Belluti F, Gobbi S, Rampa A, Valenti P, Palzer M, Paluszczak A, Hartmann RW (2001) A new class of nonsteroidal aromatase inhibitors: design and synthesis of chromone and xanthone derivatives and inhibition of the P450 enzymes aromatase and 17α-Hydroxylase/C17, 20-Lyase. J Med Chem 44:672–680

2. Nakatani K, Nakahata N, Arakawa T, Yasuda H, Ohizumi Y (2002) Inhibition of cyclooxygenase and prostaglandin E$_2$ synthesis by γ-mangostin, a xanthone derivative in mangosteen, in C6 rat glioma cells. Biochem Pharmacol 63:73–79

3. Wang LW, Kang JJ, Chen IJ, Teng CM, Lin CN (2002) Antihypertensive and vasorelaxing activities of synthetic xanthone derivatives. Bioorg Med Chem 10:567–572

4. Liu Y, Ma L, Chen WH, Wang B, Xu ZL (2007) Synthesis of xanthone derivatives with extended π-systems as α-glucosidase inhibitors: insight into the probable binding mode. Bioorg Med Chem 15:2810–2814

5. Jackson WT, Boyd RJ, Froelich LL, Gapinski DM, Mallett BE, Sawyer JS (1993) Design, synthesis, and pharmacological evaluation of potent xanthone dicarboxylic acid leukotriene B$_4$ receptor antagonists. J Med Chem 36:1726–1734

6. Hansen M, Lee SJ, Cassady JM, Hurley LH (1996) Molecular details of the structure of a psorospermin-DNA covalent/intercalation complex and associated DNA sequence selectivity. J Am Chem Soc 118:5553–5561

7. Heald RA, Dexheimer TS, Vankayalapati H, Siddiqui-Jain A, Szabo LZ, Gleason-Guzman MC, Hurley LH (2005) Conformationally restricted analogues of psorospermin: design, synthesis, and bioactivity of natural-product-related bisfuranoxanthones. J Med Chem 48:2993–3004

8. Sittisombut C, Boutefnouchet S, Van-Dufat HT, Tian W, Michel S, Koch M, Tillequin F, Pfeiffer B, Pierre A (2006) Synthesis and cytotoxic activity of benzo[a]pyrano [3, 2-h] and [2, 3-i]xanthone analogues of psorospermine, acronycine, and benzo[a]acronycine. Chem Pharm Bull 54:1113–1118

9. Woo S, Jung J, Lee C, Kwonb Y, Naa Y (2007) Synthesis of new xanthone analogues and their biological activity test-cytotoxicity, topoisomerase II inhibition, and DNA cross-linking study. Bioorg Med Chem Lett 17:1163–1166

10. Matsumoto K, Akao Y, Ohguchi K, Ito T, Tanaka T, Iinumad M, Nozawa Y (2005) Xanthones induce cell-cycle arrest and apoptosis in human colon cancer DLD-1 cells. Bioorg Med Chem 13:6064–6069

11. Zuber G Jr, Quada JC, Hecht SM (1998) Sequence selective cleavage of a DNA octanucleotide by chlorinated bithiazoles and bleomycins. J Am Chem Soc 120:9368–9369

12. Li VS, Choi D, Wang Z, Jimenez LS, Tang MS, Kohn H (1996) Role of the C-10 substituent in mitomycin C-1-DNA bonding. J Am Chem Soc 118:2326–2331

13. Liou SS, Shieh WL, Cheng TH, Won SJ, Lin CN (1993) γ-Pyrone compounds as potential anti-cancer drugs. J Pharm Pharmacol 45:791–794

14. Lin CN, Liou SS, Lee TH, Chuang YC, Won SJ (1996) Xanthone derivatives as potential anti-cancer drugs. J Pharm Pharmacol 48:539–544

15. Liu Y, Zou L, Ma L, Chen WH, Wang B, Xu ZL (2006) Synthesis and pharmacological activities of xanthone derivatives as α-glucosidase inhibitors. Bioorg Med Chem 14:5683–5690

16. Wang TC, Zhao YL, Liou SS (2002) Synthesis and cytotoxic evaluation of potential bis-intercalators:tetramethylenebis(oxy)- and hexamethylenebis(oxy)-linked assemblies consisting of flavone, xanthone, anthraquinone, and dibenzofuran. Helv Chim Acta 85:1382–1389

17. Michael TC, Marisol R, Allen JB (1989) Voltammetric studies of the interaction of metal chelates with DNA. 2. tris-chelated complexes of cobalt (III) and iron (II) with 1, 10-phenanthroline and 2, 2′-bipyridine. J Am Chem Soc 111:8901–8911

18. Kumar CV, Asuncion EH (1993) DNA binding studies and site selective fluorescence sensitization of an anthryl probe. J Am Chem Soc 115:8547–8553

19. Lippard SJ (1978) Platinum complexes: probes of polynucleotide structure and antitumor drugs. Acc Chem Res 11:211–217

20. Zeng YB, Yang N, Liu WS, Tang N (2003) Synthesis, characterization and DNA-binding properties of La(III) complex of chrysin. J Inorg Biochem 97:258–264

21. Kumar CV, Barton JK, Turro NJ (1985) Photophysics of ruthenium complexes bound to double helical DNA. J Am Chem Soc 107:5518–5523

22. Eftink MR, Ghiron CA (1981) Fluorescence quenching studies with proteins. Anal Biochem 114:199–227

23. Boger DL, Fink BE, Brunette SR, Tse WC, Hedrick MP (2001) A simple, high-resolution method for establishing DNA binding affinity and sequence selectivity. J Am Chem Soc 123:5878–5891

24. Satyanarayana S, Dabrowiak JC, Chaires JB (1992) Neither Δ-nor Λ-tris(phenanthro-line)ruthenium(II) binds to DNA by classical intercalation. Biochemistry 31:9319–9324

25. Zou XH, Ye BH, Li H, Liu JG, Xiong Y, Ji LN (1999) Mono- and bi-nuclear ruthenium(II) complexes containing a new asymmetric ligand 3-(pyrazin-2-yl)-as-triazino[5,6-f] 1,10-phenanthroline: synthesis, characterization and DNA-binding properties. J Chem Soc Dalton Trans 9:1423–1428

26. Sigman DS, Mazumder A, Perrin DM (1993) Chemical nucleases. Chem Rev 93:2295–2316

27. Eriksson M, Leijon M, Hiort C, Norden B, Gradslund A (1994) Binding of Δ- and Λ-[Ru(phen)$_3$]$^{2+}$ to [d(CGCGATCGCG)]$_2$ Studied by NMR. Biochemistry 33:5031–5040

28. Xiong Y, He XF, Zou XH, Wu JZ, Chen XM, Ji LN, Li RH, Zhou JY, Yu KB (1999) Interaction of polypyridyl ruthenium(II) complexes containing non-planar ligands with DNA. J Chem Soc Dalton Trans 1:19–23

29. Haq I, Lincoln P, Suh D, Norden B, Chowdhry BZ, Chaires JB (1995) Interaction of .Δ- and .Λ-[Ru(phen)2DPPZ]2+ with DNA: a calorimetric and equilibrium binding study. J Am Chem Soc 117:4788–4796

30. Pellegrini PP, Aldrich-Wright JR (2003) Evidence for chiral discrimination of ruthenium(II) polypyridyl complexes by DNA. Dalton Trans 2:176–183

31. Cory M, Mckee DD, Kagan J, Henry DW, Miller JA (1985) Design, synthesis, and DNA binding properties of bifunctional intercalators. Comparison of polymethylene and diphenyl ether chains connecting phenanthridine. J Am Chem Soc 107:2528–2536

32. Maheswari PU, Palaniandavar M (2004) DNA binding and cleavage properties of certain tetrammine ruthenium(II) complexes of modified 1, 10-phenanthrolines-effect of hydrogen-bonding on DNA-binding affinity. J Inorg Biochem 98:219–230

33. Dupureur CM, Barton JK (1997) Structural studies of Λ- and Δ-[Ru(phen)2d ppz]2+ bound to d(GTCGAC)2: characterization of enantioselective intercalation. Inorg Chem 36:33–43

34. Neyhart GA, Grover N, Smith SR, Kalsbeck WA, Fairley TA, Cory M, Thorp HH (1993) Binding and kinetics studies of oxidation of DNA by oxoruthenium(IV). J Am Chem Soc 115:4423–4428